Amplification and propagation of pacemaker Ca^{2+} signals by cyclic ADP-ribose and the type 3 ryanodine receptor in T cells

Svenja Kunerth[1], Matthias F. Langhorst[1], Nadine Schwarzmann[1,*], Xianfeng Gu[2], Lijun Huang[2], Zhenjun Yang[2], Liangren Zhang[2], Steven J. Mills[3], Li-he Zhang[2], Barry V.L. Potter[3] and Andreas H. Guse[1,‡]

[1]University Hospital Hamburg-Eppendorf, Center for Experimental Medicine, Institute of Biochemistry and Molecular Biology I: Cellular Signal Transduction, Martinistr. 52, 20246 Hamburg, Germany
[2]National Laboratory of Natural and Biomimetic Drugs, School of Pharmaceutical Sciences, Peking University, 38 Xue Yuan Road, Beijing 100083, China
[3]Wolfson Laboratory of Medicinal Chemistry, Department of Pharmacy and Pharmacology, University of Bath, Claverton Down, Bath, BA2 7AY, UK
*Present address: AstraZeneca, Tinsdaler Weg 183, 22876 Wedel, Germany
‡Author for correspondence (e-mail: guse@uke.uni-hamburg.de)

Accepted 17 December 2003
Journal of Cell Science 117, 2141-2149 Published by The Company of Biologists 2004
doi:10.1242/jcs.01063

Summary

Ligation of the T-cell receptor/CD3 complex results in global Ca^{2+} signals that are essential for T-cell activation. We have recently reported that these global Ca^{2+} signals are preceded by localized pacemaker Ca^{2+} signals. Here, we demonstrate for the first time for human T cells that an increase in signal frequency of subcellular pacemaker Ca^{2+} signals at sites close to the plasma membrane, in the cytosol and in the nucleus depends on the type 3 ryanodine receptor (RyR) and its modulation by cyclic ADP-ribose. The spatial distribution of D-*myo*-inositol 1,4,5-trisphosphate receptors and RyRs indicates a concerted action of both of these receptors/Ca^{2+} channels in the generation of initial pacemaker signals localized close to the plasma membrane. Inhibition or knockdown of RyRs resulted in significant decreases in (1) the frequency of initial pacemaker signals localized close to the plasma membrane, and (2) the frequency of localized pacemaker Ca^{2+} signals in the inner cytosol. Moreover, upon microinjection of cyclic ADP-ribose or upon extracellular addition of its novel membrane-permeant mimic *N*-1-ethoxymethyl-substituted cyclic inosine diphosphoribose, similarly decreased Ca^{2+} signals were observed in both type 3 RyR-knockdown cells and in control cells microinjected with the RyR antagonist Ruthenium Red. Taken together, our results show that, under physiological conditions in human T cells, RyRs play crucial roles in the local amplification and the spatiotemporal development of subcellular Ca^{2+} pacemaker signals.

Key words: Ca^{2+} signaling, Ryanodine receptor, Cyclic ADP-ribose, T cell, D-*myo*-inositol 1,4,5-trisphosphate receptor

Introduction

Subcellular Ca^{2+} signals are the fundamental pacemaking events preceding global Ca^{2+} waves and/or Ca^{2+} oscillations. These global Ca^{2+} signals are then converted into cellular responses such as cell proliferation, differentiation, fertilization, exocytosis and muscle contraction (reviewed by Guse 2000; da Silva and Guse, 2000; Galione and Churchill, 2002; Guse, 2002; Berridge et al., 2003). The different phases of the development of the cellular Ca^{2+} signal were described as (1) the basal phase, (2) the pacemaker phase, in which subcellular Ca^{2+} signals were observed, and (3) the global signal (Bootman et al., 1997a). Subcellular Ca^{2+} signals during the pacemaker phase were analyzed in several non-excitable and excitable cell types (Thorn et al., 1993; Tsugorka et al., 1995; Yao et al., 1995; Lipp and Niggli, 1996; Klein et al., 1996; Thomas et al., 2000; Tovey et al., 2001).

The molecular mechanisms underlying subcellular Ca^{2+} signals were analyzed by stimulation of cells with agonists that are thought exclusively, or at least mainly, to stimulate one of the intracellular systems for Ca^{2+} mobilization; for example, histamine to stimulate the D-*myo*-inositol 1,4,5-trisphosphate [Ins(1,4,5)P_3]/Ca^{2+}-signaling pathway (Bootman et al., 1997b) or caffeine to stimulate exclusively the ryanodine receptor (RyR) (Conklin et al., 1999; Rossi et al., 2002). However, the assumption that exclusive stimulation of one of the Ca^{2+}-mobilizing systems is experimentally possible is problematic for two reasons. First, in a growing number of cell types, more than one system is functionally expressed (reviewed by da Silva and Guse, 2000; Yusufi et al., 2002). Second, the D-*myo*-Ins(1,4,5)P_3 receptor (D-*myo*-Ins(1,4,5)P_3R) and the RyR might respond to [Ca^{2+}] elevations by Ca^{2+}-induced Ca^{2+} release (CICR) and thus could be recruited even if the primary effect was targeted to one of the other systems for Ca^{2+} mobilization (reviewed by Galione and Churchill, 2002).

Recently, we generated and thoroughly characterized a type 3 RyR-knockdown Jurkat T-cell clone (Schwarzmann et al., 2002). In this clone, RyR expression was substantially decreased whereas Ins(1,4,5)P_3R expression remained unchanged. At both the cell-population level and the single-cell level, reduced Ca^{2+} signaling was observed during the

long-lasting phase following T-cell receptor (TCR)/CD3 complex stimulation (Schwarzmann et al., 2002). Using the membrane-permeant cyclic ADP-ribose (cADPR) antagonist 7-deaza-8-Br-cADPR, we showed earlier that cADPR is a major player in the sustained Ca^{2+}-signaling phase (Guse et al., 1999). Thus, one major system acting in the long-lasting Ca^{2+}-signaling phase is the cADPR/type 3 RyR/Ca^{2+}-signaling system.

However, in addition to its inhibitory effect in the sustained Ca^{2+}-signaling phase, 7-deaza-8-Br-cADPR also delayed the onset of the global Ca^{2+} signal upon stimulation of the TCR/CD3 complex (Guse et al., 1999), indicating that in addition to its role in the sustained phase the cADPR/type 3 RyR/Ca^{2+}-signaling system might play a crucial role during the pacemaker phase, which is the phase between stimulation of the TCR/CD3 complex and the first global Ca^{2+} signal. To test this hypothesis, pacemaker Ca^{2+} signals were comprehensively analyzed in type 3 RyR-deficient Jurkat T-cell clones stimulated through the TCR/CD3 complex, by microinjection of cADPR or by extracellular addition of a novel membrane-permeant cADPR mimic, *N*-1-ethoxymethyl-substituted cyclic inosine diphosphoribose (cIDPRE).

Materials and Methods

Materials

Fetal calf serum (tetracycline-free) was obtained from Biochrom. Fura-2/AM, anti-Ins(1,4,5)*P*$_3$R rabbit antiserum and ionomycin were purchased from Calbiochem. The anti-CD3 mouse monoclonal antibody (mAb) OKT3 was purified from hybridoma supernatant on Protein G-Sepharose FF (Amersham Pharmacia Biotech). Anti-Ins(1,4,5)*P*$_3$R subtype-specific polyclonal antisera and blocking peptides were purchased from Santa Cruz Biotechnology. Ruthenium Red X-conjugated goat anti-rabbit secondary antibody was obtained from Dianova. Hoechst Stain 33258, BODIPY FL thapsigargin, Alexa568-conjugated rabbit anti-goat antiserum and BODIPY FL-X ryanodine were obtained from Molecular Probes Europe.

Synthesis of *N*-1-ethoxymethyl-substituted cyclic inosine diphosphoribose (cIDPRE)

Experiments in intact and permeabilized Jurkat T cells showed that cIDPRE is a membrane-permeant mimic of cADPR (e.g. extracellular addition of cIDPRE resulted in sustained Ca^{2+} signaling in the presence of extracellular Ca^{2+}, whereas in its absence a transient Ca^{2+} response was obtained). In permeabilized cells, cIDPRE released Ca^{2+} from the same pool as compared with cADPR, but its activity was somewhat weaker. Full synthetic details and full pharmacological characterization of cIDPRE will be published elsewhere. cIDPRE was synthesized from *N*-1-acetoxyethoxymethyl-substituted inosine using the similar seven steps described for the synthesis of *N*-1-glycosyl-substituted cyclic IDP-ribose derivatives (Huang et al., 2002a; Huang et al., 2002b). The synthetic compound was identified by ^{1}H and ^{31}P nuclear magnetic resonance (NMR) spectroscopy and mass spectroscopy after purification twice by high-performance liquid chromatography (HPLC). The compound was used as its triethylammonium salt.

Synthesis of D-*myo*-inositol 1,4,6-trisphosphorothioate [D-Ins(1,4,6)*P*S$_3$]

D-Ins(1,4,6)*P*S$_3$ was synthesized from 1D-2,3,5-tri-*O*-benzyl *myo*-inositol (Mills and Potter, 1996) using methods similar to those described for the racemic mixture (Mills et al., 1995). All synthetic compounds were homogenous by ^{1}H and ^{31}P NMR spectroscopy and mass spectroscopy after purification by ion-exchange chromatography. The compounds were quantified by total phosphate assay and then used as their triethylammonium salts. D-Ins(1,4,6)*P*S$_3$ was evaluated biologically and shown to be a low-efficiency partial agonist at the Ins(1,4,5)P$_3$R (Murphy et al., 2000) and to antagonize Ins(1,4,5)P$_3$-induced Ca^{2+} release.

Cell culture

Jurkat T cells (clone JMP) were cultured as described (Guse et al., 1993). Tet-On Jurkat T-cell clone E2 (abbreviated E2) and clone 25 (abbreviated 25) were cultured in RPMI 1640 supplemented with Glutamax I, 10% (v/v) fetal calf serum (free of tetracycline; Biochrom), 25 mM HEPES, 1 mM sodium pyruvate, 100 units/ml penicillin, 50 μg/ml streptomycin, 50 μg/ml hygromycin and 400 μg/ml G418-Sulfat (Schwarzmann et al., 2002).

Ratiometric Ca^{2+} imaging

The cells were loaded with Fura-2/AM as described (Guse et al., 1993) and kept in the dark at room temperature until use. The coating of the glass coverslips was done with BSA (5 mg/ml), and poly-L-lysine (0.1 mg/ml). Small chamber slides consisting of a rubber O-ring were sealed on thin (0.1 mm) glass coverslips by silicon grease. Then, 60 μl buffer A containing 140 mM NaCl, 5 mM KCl, 1 mM $MgSO_4$, 1 mM $CaCl_2$, 1 mM NaH_2PO_4, 5.5 mM glucose and 20 mM HEPES (pH 7.4), and 40 μl cell suspension (2×10^6 cells/ml) suspended in the same buffer were added into the small chamber (Berg et al., 2000). Then, the coverslip was mounted on the stage of a fluorescence microscope (Leica DM IRE2).

Ratiometric Ca^{2+} imaging was performed as described in an earlier report (Kunerth et al., 2003). In brief, an Improvision imaging system built around the Leica microscope at 100-fold magnification was used. Illumination at 340 and 380 nm was carried out using a monochromator system (Polychromator IV, TILL Photonics). Images were taken with a gray-scale CCD camera (type C4742-95-12ER; Hamamatsu; operated in 8-bit mode) on three consecutive horizontal (z) planes, each 0.5 μm from the focal plane up and down. The optimal relation of spatial to temporal resolution for the ratiometric measurements was obtained using a spatial resolution of 512×640 pixel, resulting in a pixel length of 129 nm/pixel (at 100-fold magnification). The maximal acquisition rate was 0.5 seconds for three pairs of images (340 and 380 nm, one pair in each of the three horizontal planes). Raw data images were stored on hard disk. To obtain digital confocal images, mathematical deconvolution based on the point-spread function was carried out using the nearest-neighbor algorithm (Openlab software v3.0.9, Improvision). The pinhole was set to 50% removal of stray light. After deconvolution of the raw data, confocal ratio images (340/380) were constructed pixel by pixel and, finally, ratio values were converted to Ca^{2+} concentrations by external calibration. To reduce noise, ratio images were subjected to median filter (3×3) as described (Kunerth et al., 2003).

Localization of Ca^{2+}-signaling proteins

The SERCA ATPases of intact cells were stained with 1 μM BODIPY FL thapsigargin for 30 minutes at room temperature in the dark. Control cells were incubated with 100 μM thapsigargin and 1 μM BODIPY thapsigargin. For the staining of the TCR/CD3 complex, the cells were fixed (but not permeabilized) using 2% (w/v) p-formaldehyde in buffer A for 15 minutes at room temperature. Then the cells were rinsed twice with buffer A. Afterwards, the cells were incubated for 60 minutes at room temperature with 1 μg OKT3/100 μl, washed twice with buffer A and finally incubated for 60 minutes at room temperature with FITC-conjugated goat anti-mouse secondary antibody in the dark. For staining of Ca^{2+}-signaling proteins, the cells were fixed using 2% (w/v) p-formaldehyde in buffer

A (see above) for 15 minutes at room temperature and washed twice with buffer A. The cells were permeabilized with methanol (5 minutes at room temperature) and rinsed again twice with buffer A. The cells were then incubated with anti-Ins(1,4,5)P_3R antibody at 1 μg/100 μl for 60 minutes at room temperature. The antibody was then removed by two subsequent washing steps. Finally, a Rhodamine-conjugated rabbit anti-goat secondary antibody was added at 4 μg/100 μl for 60 minutes at room temperature in the dark. Controls were carried out using Rhodamine-conjugated rabbit anti-goat secondary antibody only. The RyR was stained with 25 μM BODIPY FL-X ryanodine for 2 hours at room temperature in the dark. Control cells were stained in the presence of tenfold surplus ryanodine. After the incubation step, the secondary antibody or BODIPY FL-X ryanodine was removed by three washing steps. The nucleus was stained by treatment with 0.1 μg/μl H33258 for 15 minutes at room temperature in the dark. Then, 100 μl of the cell suspension was mounted on a glass coverslip as described above.

Confocal microscopy was performed using the Improvision imaging system as described above. Images were taken on 10-50 consecutive horizontal planes (z), at a step width of 0.2 μm. The spatial resolution in each horizontal plane (xy) was 67 nm/pixel at 100-fold magnification. Raw data images were stored on hard disk. Mathematical deconvolution based on the point-spread function was carried out using three or more neighbors on each side of the central horizontal z-plane of the cell. The magnitude setting for removal of stray light was set between 23% and 68%.

Microinjection

Microinjections were done as described (Guse et al., 1997). Briefly, we used an Eppendorf system (transjector type 5246, micromanipulator type 5171; Eppendorf-Netheler-Hinz) with Femtotips II as pipettes. cADPR was diluted to its final concentration in intracellular buffer (20 mM HEPES, 110 mM KCl, 2 mM $MgCl_2$, 5 mM KH_2PO_4, 10 mM NaCl, pH 7.2) and filtered (0.2 μm) before use. Injections were made using the semiautomatic mode of the system with the following instrumental settings: injection pressure 60 (Jurkat T cell) or 40 hPa (clones E2 and 25); compensatory pressure 30 (Jurkat T cell) or 25 hPa (clones E2 and 25); injection time 0.5 (Jurkat T cell) or 0.3 seconds (clones E2 and 25); and velocity of the pipette 700 μm/second. Under such conditions, the injection volume was 1-1.5% of the cell volume (Guse et al., 1997).

Results

To understand the role of the type 3 RyR in early global Ca^{2+} signaling, the established type 3 RyR-knockdown Jurkat T-cell clone 25 (Fig. 1b) was analyzed comprehensively versus the control clone E2 (Fig. 1a) (Schwarzmann et al., 2002). The type 3 RyR-knockdown clone 25 was obtained by stable transfection with the type 3 RyR antisense plasmid pTRE2-511, whereas the control clone E2 was stably transfected with the control plasmid pTRE2-EGFP (Schwarzmann et al., 2002). Anti-CD3 mAb OKT3 induced a rapid bi-phasic Ca^{2+} signal in the control clone E2 (Fig. 1a), whereas a delayed onset and a slightly reduced Ca^{2+} peak was observed in the type 3 RyR-knockdown clone 25 (Fig. 1b). Microinjection of the RyR antagonist Ruthenium Red (RuRed) partially blocked TCR/CD3-mediated Ca^{2+} signaling in clone E2; specifically, the onset of the global signal was largely delayed (Fig. 1c). Microinjection of the Ins(1,4,5)P_3 antagonist D-Ins(1,4,6)PS_3 completely blocked the Ca^{2+} signal upon TCR/CD3 ligation in clone E2 (Fig. 1d) as described earlier (Guse et al., 1999). These results confirm our previous model that Ins(1,4,5)P_3 is essential for onset of Ca^{2+} signaling upon TCR/CD3

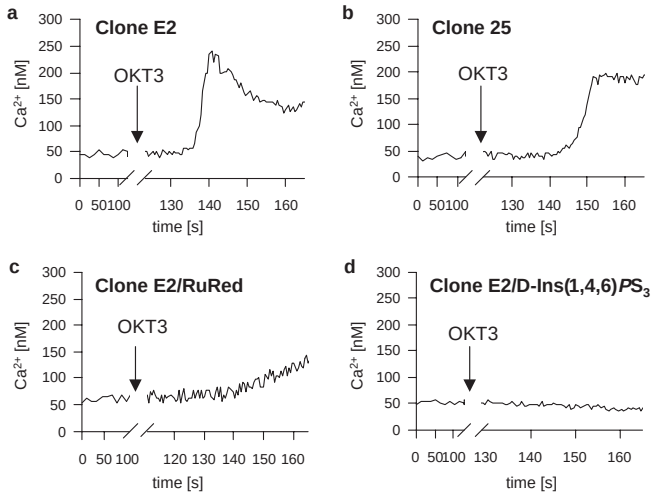

Fig. 1. Effect of type 3 RyR knockdown, RyR inhibition and Ins(1,4,5)P_3R inhibition on early global Ca^{2+} signaling upon TCR/CD3 ligation. T cells [control clone E2 (a,c,d) or type 3 RyR-knockdown clone 25 (b)] were loaded with Fura-2/AM and analyzed by single-cell Ca^{2+} imaging as described in the Materials and Methods. OKT3 was added to a final concentration of 10 μg/ml as indicated. Inhibitors were microinjected directly before start of the measurement: (c) Ruthenium Red (RuRed; pipette concentration 10 μM), (d) D-Ins(1,4,6)PS_3 (pipette concentration 80 μM). Data acquisition rate was 0.1 ratios/second before OKT3 addition, and 2 ratio/second thereafter. Characteristic tracings out of 18-39 cells are displayed.

stimulation, but also indicate that RyRs play an important modulatory role in the early pacemaker phase.

This role of RyRs was then analyzed in detail by confocal Ca^{2+} imaging (Fig. 2). First, the reduction of RyR expression in clone 25 was confirmed using staining by BODIPY FL-X ryanodine (Fig. 2Aa versus Ba). The expression of Ins(1,4,5)P_3R was unchanged in clone 25 versus clone E2 (Schwarzmann et al., 2002). Fura-2-loaded T cells were then stimulated using solid-phase-bound anti-CD3 antibody OKT3. The pseudocolor Ca^{2+} images shown in Fig. 2Ab and Bb were taken in the pacemaker phase and demonstrate the difference in amplitude and distribution of local Ca^{2+} signals. Analysis of the temporal development of such pacemaker signals in three different subcellular regions of interest (ROIs) characteristic for the cell border (edge), cytosol or nucleus, as indicated in Fig. 2Ab and Bb, revealed comparable signal amplitudes, but a reduced number of signals in the cytosol in type 3 RyR-knockdown cells as compared with control cells (Fig. 2Ab versus Bb, right panels). This type of analysis was extended to control cells microinjected with RuRed or D-Ins(1,4,6)PS_3 before stimulation by OKT3 (data summarized in Fig. 2C,D). The amplitude of Ca^{2+} signals slightly decreased when comparing the cell border versus cytosol or nucleus, but at the same subcellular region the amplitudes remained almost unchanged among all conditions tested (Fig. 2C). By contrast, a significant decrease in the frequency of Ca^{2+} signals was observed in all three regions in cells previously microinjected by RuRed (Fig. 2D). Interestingly, in type 3 RyR-knockdown clone 25, a reduction of the Ca^{2+} signal frequency was only observed in the cytosol, but not at the cell border or in the nucleus (Fig. 2D). Thus, the pan-RyR antagonist RuRed

reduces the frequency also at those sites (cell border, nucleus) where type 3 RyRs do not appear to play a major role, indicating either expression of additional RyR subtypes in T cells or additional targets for the drug RuRed. As expected, the Ins(1,4,5)P_3 antagonist D-Ins(1,4,6)PS_3 reduced the frequency, but not the amplitude, in all subcellular regions to a similar extend as RuRed (Fig. 2D). Taken together, these data indicate that RyRs in general, and type 3 RyRs specifically in the cytosol, significantly contribute to the amplification of early pacemaker signals by increasing the signal frequency.

Previously, we showed that cADPR activates Ca^{2+} release through the type 3 RyR and that cADPR is essentially involved in the sustained phase of Ca^{2+} signaling in T cells (Schwarzmann et al., 2002; Guse et al., 1999). To investigate a potential role for cADPR also in the development of pacemaker Ca^{2+} signals, a similar analysis as described in Figs 1 and 2 was conducted. Instead of stimulating the cells through the TCR/CD3 complex, microinjection of cADPR or extracellular addition of a novel membrane-permeant cADPR mimic, cIDPRE, was carried out to stimulate the RyRs. The global Ca^{2+} signal upon microinjection of a moderate concentration of cADPR (20 μM) activated a typical global Ca^{2+} signal with a delayed onset and a moderate amplitude in the control clone E2 (Fig. 3a). By contrast, in the type 3 RyR-knockdown clone 25, the global signal was almost absent and, if present at all, occurred after a very long delay (Fig. 3b). Extracellular addition of a high concentration (500 μM) of the membrane-permeant cADPR mimic cIDPRE activated a rapid and sustained Ca^{2+} signal that was almost completely suppressed by previous injection of RuRed (Fig. 3c). Moreover, the onset and amplitude of the cIDPRE-mediated signal was largely delayed and reduced in the type 3 RyR-knockdown clone 25 (Fig. 3d). These data clearly show that elevation of cADPR without ligation of the TCR/CD3 complex activates global Ca^{2+} signaling in T cells.

Confocal Ca^{2+} imaging of the pacemaker phase resulted in the detection of local Ca^{2+} signals at the cell border (edge), in the cytosol, and to a lesser extent in the nucleus (Fig. 4A,B). The number of Ca^{2+} signals was markedly reduced in the cytosol of the type 3 RyR-knockdown clone 25 as compared

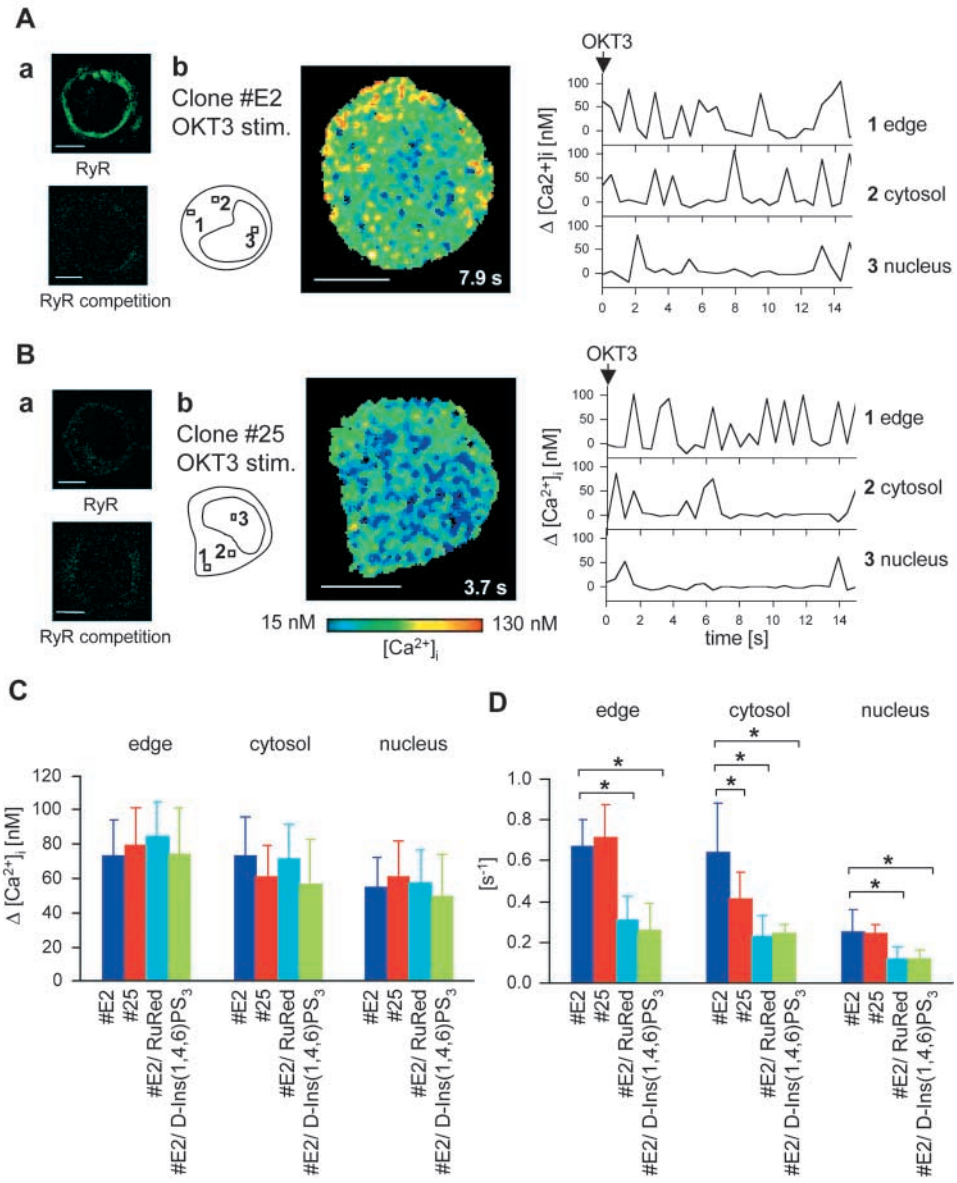

Fig. 2. Effect of type 3 RyR knockdown, RyR inhibition and Ins(1,4,5)P_3R inhibition on early local Ca^{2+} signaling upon TCR/CD3 ligation. T cells [control clone E2 (A) or type 3 RyR-knockdown clone 25 (B)] were loaded with Fura-2/AM and analyzed by single-cell confocal Ca^{2+} imaging as described in the Materials and Methods. OKT3 (final concentration 10 μg/ml) was added as indicated (Ab,Bb). Inhibitors were microinjected directly before start of the measurement: Ruthenium Red (RuRed; pipette concentration 10 μM), D-Ins(1,4,6)PS_3 (pipette concentration 80 μM). Data acquisition rate was 0.1 ratios/second before OKT3 addition, and 2 ratios/second thereafter. Staining for RyR expression was performed using BODIPY FL-X-ryanodine (Aa,Ba). Characteristic confocal ratio Ca^{2+} images acquired in the pacemaker phase are displayed (Ab,Bb; bar, 5 μm) and amplitudes of selected ROIs (see inset) are plotted against time for a 15-second time interval. Data in C and D are presented as mean±s.d. [n=9 ROIs for each subcellular region (edge, cytosol, nucleus) taken from three different individual cells]. Asterisks denote significant differences as indicated (P≤0.05, Student's t test).

with clone E2 (Fig. 4A,B). Detailed analysis of the pacemaker Ca^{2+} signals upon cADPR microinjection or cIDPRE addition revealed interesting parallels to the stimulation of the TCR/CD3 complex. First, the mean amplitudes slightly decreased from the edge via the cytosol to the nucleus (Fig. 4C). Second, no significant differences were detected in the amplitudes of Ca^{2+} signals within each of the three subcellular regions, regardless of whether microinjection of cADPR was compared between the clones 25 and E2, or whether extracellular addition of cIDPRE in clone E2 was compared with type 3 RyR-knockdown clone 25 or with control clone E2 previously microinjected with RuRed (Fig. 4C). In contrast to the amplitudes, and in a similar way as for TCR/CD3 stimulation (see Fig. 2), the frequency of cADPR- or cIDPRE-induced pacemaker Ca^{2+} signals in the cytosol was significantly reduced in either the type 3 RyR-knockdown clone 25 or in the control clone E2 previously microinjected with RuRed (Fig. 4D). In addition, a significant difference was also observed in the nucleus upon microinjection of cADPR (Fig. 4D). Taken together, these data indicate that, upon TCR/CD3 ligation, cADPR and the type 3 RyRs are important amplifiers of local pacemaker Ca^{2+} signals; they act together by increasing the frequency of local Ca^{2+} signals in the cytosol.

Comprehensive microinjection of Ins(1,4,5)P_3 into the control clone E2 versus the type 3 RyR-knockdown clone 25 resulted in a somewhat reduced global Ca^{2+} peak (Fig. 5a,b). Similar results were obtained by comparing the microinjection of Ins(1,4,5)P_3 versus the combined injection of Ins(1,4,5)P_3/RuRed (Fig. 5c,d). These data confirm that injection of a high concentration of Ins(1,4,5)P_3 on its own induces global Ca^{2+} signals in T cells (Guse et al., 1997), but also indicate that, even if Ins(1,4,5)P_3R are fully engaged, there is still a small amplificatory effect of RyRs.

To correlate spatially the subcellular Ca^{2+} signals with the receptors for the Ca^{2+}-releasing second messengers Ins(1,4,5)P_3 and cADPR, the Ins(1,4,5)P_3R and the RyR were stained in p-formaldehyde-fixed and permeabilized cells. The Ins(1,4,5)P_3R was localized close to the plasma membrane and showed a spot-like staining (Fig. 6C). A similar distribution was detected for each of the three Ins(1,4,5)P_3R subtypes (not shown). Also, the RyR was found close to the plasma membrane, but at a lower density that also extended further into the inner cytosol (Fig. 6B). The arrangement of plasma membrane, nucleus and endoplasmic reticulum (ER), visualized by CD3 staining in intact cells, Hoechst nuclear stain and sarcoplasmic/endoplasmic reticulum ATPase (SERCA) staining by BODIPY-thapsigargin in permeabilized cells, is depicted in Fig. 6D,E,F, respectively. Upon OKT3 stimulation, no significant change in the distribution of these proteins or organelles was observed, except a somewhat enhanced clustering of CD3 (not shown). The distribution of the Ins(1,4,5)P_3R versus RyR indicates that mixed groups consisting of both receptors are expressed close to the plasma membrane at specific sites. These groups appear to initiate Ca^{2+} signaling in T cells because local Ca^{2+} signals close to the plasma membrane are observed at early time points during the pacemaker phase (Fig. 6A), and inhibition of both the Ins(1,4,5)P_3R and RyR resulted in significant decreases in signal frequency (Fig. 2D). Ca^{2+} signal frequency in the inner parts of the cytosol upon TCR/CD3 ligation was greatly reduced in type 3 RyR-knockdown T cells (Fig. 2D), a finding that correlates well with the staining of RyRs (Fig. 6B).

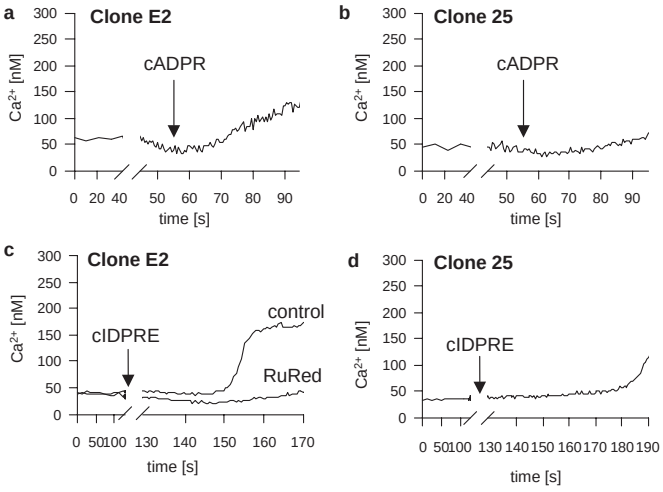

Fig. 3. Effect of type 3 RyR knockdown or RyR inhibition on global Ca^{2+} signaling upon activation of the cADPR/Ca^{2+}-signaling system. T cells [control clone E2 (a,c) or type 3 RyR-knockdown clone 25 (b,d)] were loaded with Fura-2/AM and analyzed by single-cell Ca^{2+} imaging as described in the Materials and Methods. cADPR was microinjected (a,b; pipette concentration 20 μM) or cIDPRE was added extracellularly (c,d; final concentration 500 μM) as indicated. Inhibitors were microinjected directly before start of the measurement: (c) Ruthenium Red (RuRed; pipette concentration 10 μM). Data acquisition rate was 0.1 ratios/second before OKT3 addition, and 2 ratios/second thereafter. Characteristic tracings out of 15-24 cells are displayed.

Discussion

Here we report for the first time for human T cells that the spatiotemporal amplification of subcellular pacemaker Ca^{2+} signals depends on the type 3 RyR and its modulation by cADPR. In particular, it is demonstrated that: (1) both inhibition or knockdown of RyR in cells stimulated through the TCR/CD3 complex significantly reduced the frequency of local Ca^{2+} signals, resulting in delayed and decreased global Ca^{2+} signals; (2) upon microinjection of cADPR or extracellular addition of the novel membrane-permeant cADPR mimic cIDPRE (instead of stimulation of the TCR/CD3 complex), similar differences as for TCR/CD3 ligation were observed; and (3) the spatial distribution of Ins(1,4,5)P_3R and RyR points towards a model consisting of a concerted action of both Ins(1,4,5)P_3R and RyR in the initiation of early pacemaker signals at sites close to the plasma membrane, whereas temporal amplification of local signals in the inner cytosol appears to depend mainly on RyR.

These results might be explained by the following model: upon stimulation of T cells through the TCR/CD3 complex, Ins(1,4,5)P_3 is rapidly formed (Guse et al., 1995) and cADPR increases more slowly (Guse et al, 1999). Opening of Ins(1,4,5)P_3R close to the site of Ins(1,4,5)P_3 production results in local Ca^{2+} signals; expression of Ins(1,4,5)P_3R is crucial for this process as knockdown of the type 1 Ins(1,4,5)P_3R prevented the activation of global Ca^{2+} signaling in Jurkat T cells (Jayaraman et al., 1995). The latter finding was confirmed recently (Guse et al., 1999) and also in the

present study, as blocking of Ins(1,4,5)P_3R by D-Ins(1,4,6)PS_3 largely decreased the frequency of local Ca^{2+} signals and the amplitude of global Ca^{2+} signals (Fig. 2D,1d). Since RuRed reduced the frequency of Ca^{2+} signals at the cell border to a similar extent as D-Ins(1,4,6)PS_3 (Fig. 2D), the local Ca^{2+} signals generated by Ins(1,4,5)P_3R were locally amplified by RyR. The latter are positively modulated by Ca^{2+}-induced Ca^{2+} release (CICR; Ca^{2+} released via Ins(1,4,5)P_3R), cADPR (produced upon TCR/CD3 ligation; Guse et al., 1999) and tyrosine phosphorylation (Guse et al., 2001). Interestingly, knockdown of the type 3 RyR did not result in a reduced frequency of Ca^{2+} signals at the cell border (Fig. 2D), indicating that other RyR subtypes are involved in this process. Indeed, expression of mRNA of the type 1 and 2 RyR was detected by sensitive nested RT-PCR in Jurkat T cells (N.S. and A.H.G., unpublished); however, because no subtype-specific anti-human antibodies are available at present, confirmation of expression on the protein level awaits further clarification in the future. Comprehensive microinjection of Ins(1,4,5)P_3 into control versus type 3 RyR-knockdown cells resulted in subtle differences in global Ca^{2+} signaling; likewise, upon co-injection of RuRed, Ca^{2+} signaling by Ins(1,4,5)P_3 was decreased. This indicates that, at a high Ins(1,4,5)P_3 concentration, once a certain threshold of $[Ca^{2+}]_i$ has been reached, Ins(1,4,5)P_3R on their own are sufficient to develop a global Ca^{2+} signal, but recruitment of RyR by CICR is necessary for a full response. Nevertheless, under physiological conditions (TCR/CD3 ligation) RyRs act as temporal amplifiers of the local Ca^{2+} signals. The Ca^{2+}-release events close to the plasma membrane could be further amplified locally by Ca^{2+}entry.

For spatial propagation of the pacemaker Ca^{2+} signals through the cytosol towards the nucleus, RyRs are crucial for increasing the frequency of local Ca^{2+}-release events in the inner parts of the cytosol (Fig. 2C). In contrast to the situation at the cell border, the knockdown of the type 3 RyR and inhibition by RuRed resulted in a similar phenotype (reduced frequency of local Ca^{2+} signals) in the inner cytosol, indicating that the type 3 RyR is the major RyR in this part of the cell. Although a significant reduction of the Ca^{2+} signal frequency was obtained in the type 3 RyR-knockdown cells or upon microinjection of RuRed (Fig. 2D), local Ca^{2+} signals were still observed. Because this basal activity of local Ca^{2+} signals was also present upon D-Ins(1,4,6)PS_3 injection, and also at a similar frequency in unstimulated control or RyR-knockdown cells [clone E2 0.4±0.16 (n=54; edge), 0.25±0.06 (n=34; cytosol), 0.15±0.06 (n=20; nucleus); clone 25 0.46±0.09 (n=62; edge), 0.31±0.10 (n=42; cytosol), 0.16±0.05 (n=21; nucleus)], it is likely to represent a basic local signaling system reflecting excitability of the cells, and is insensitive to the inhibitors used in this study.

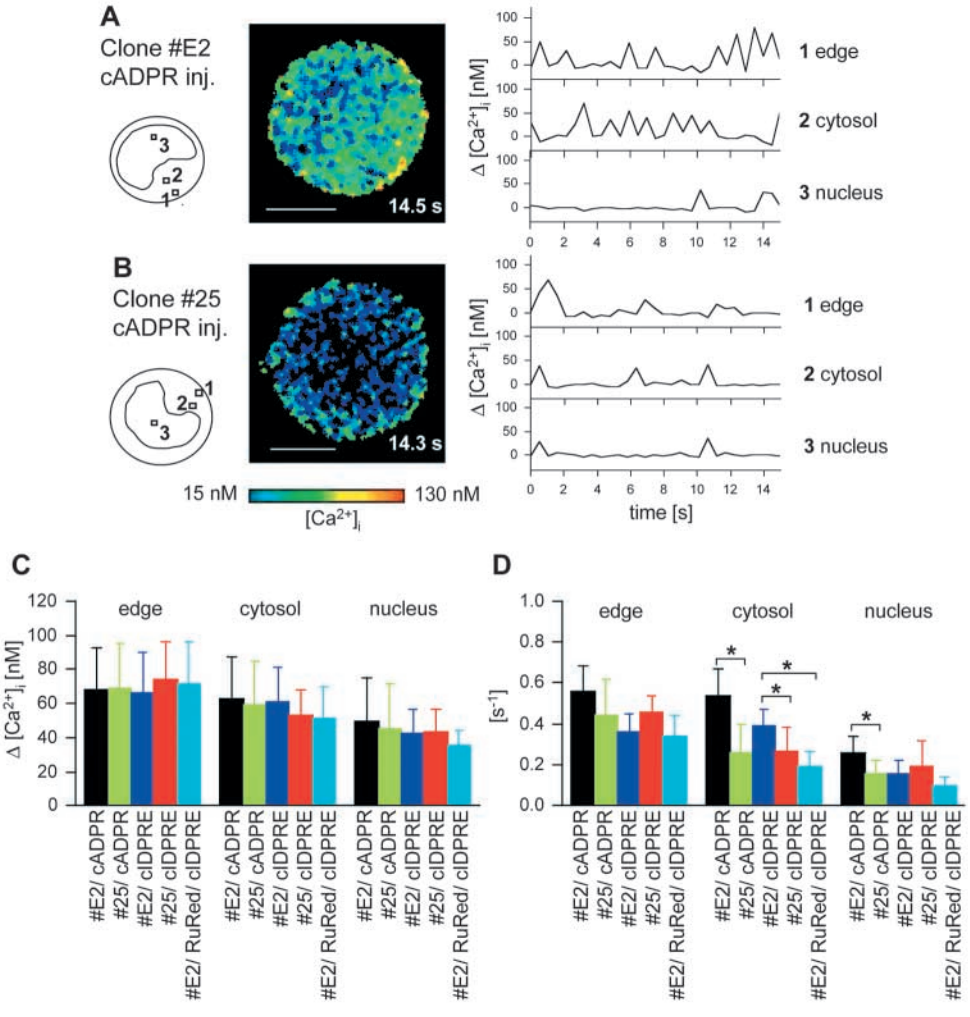

Fig. 4. Effect of type 3 RyR knockdown, RyR inhibition and Ins(1,4,5)P_3R inhibition on early local Ca^{2+} signaling upon activation of the cADPR/Ca^{2+}-signaling system. T cells [control clone E2 (A) or type 3 RyR-knockdown clone 25 (B)] were loaded with Fura-2/AM and analyzed by single-cell confocal Ca^{2+} imaging as described in the Materials and Methods. Either cADPR was microinjected (pipette concentration 20 μM) or cIDPRE was added extracellularly (final concentration 500 μM). During a 15-second time interval, characteristic confocal ratio Ca^{2+} images acquired in the pacemaker phase are displayed (A,B; bar, 5 μm) and amplitudes of selected ROIs (see inset) are plotted. Ruthenium Red (RuRed; pipette concentration 10 μM) was microinjected directly before start of the measurement. Data acquisition rate was 0.1 ratios/second before cADPR microinjection or cIDPRE addition, and 2 ratios/second thereafter. Data in C and D are presented as mean±s.d. [n=9 ROIs for each subcellular region (edge, cytosol, nucleus) taken from three different individual cells]. Asterisks denote significant differences as indicated (P≤0.05, Student's t test).

In the nucleus, the situation resembles more the one at the cell border as inhibition by RuRed had a significant effect on signal frequency whereas knockdown of the type 3 RyR did not (Fig. 2D). The fact that D-Ins(1,4,6)*P*S$_3$, in addition to its effect at the cell border, also blocked the Ca^{2+} signals more deeply within the cytosol strongly indicates that Ca^{2+} release by Ins(1,4,5)*P*$_3$ under physiological conditions is indeed the primary event.

A comparable initial role for Ins(1,4,5)*P*$_3$-mediated Ca^{2+} release was described in HeLa cells; similar to our results, a minimum threshold $[Ca^{2+}]_i$ had to be passed for the development of a global Ca^{2+} signal (Bootman et al., 1997a). In the type 3 RyR-knockdown clone, such initial Ca^{2+}-release events after TCR/CD3 stimulation were still visible (Fig. 2). Together with recent data (Jayaraman et al., 1995; Guse et al., 1999), this underpins the crucial role for Ins(1,4,5)*P*$_3$-mediated local Ca^{2+} signals as initiating events. Regarding the initiation and propagation of subcellular Ca^{2+} signals via the cytosol towards inner regions of HeLa cells activated by histamine, one group has mainly focused on the Ins(1,4,5)*P*$_3$-signaling pathway as the underlying mechanism (Bootman et al., 1997a; Bootman et al., 1997b). By contrast, in T cells stimulated through the TCR/CD3 complex, both local initiation and propagation of localized Ca^{2+} signals additionally require the type 3 RyR, and most probably its activation by cADPR.

The role of type 3 RyR has been investigated in different cell types. Overexpressing the type 3 RyR in HEK 293 cells resulted in a unique phenotype because, in contrast to overexpression of the type 1 RyR, spontaneous subcellular Ca^{2+}-release events (sparks) were observed (Rossi et al., 2002). Similarly, in 1B5 myotubes overexpressing type 3 RyR, Ca^{2+} sparks were recorded, whereas in wild-type 1B5 myotubes lacking RyR, sparks were not observed (Ward et al., 2000). However, Estrada et al. reported that wild-type 1B5 myotubes still respond to depolarization, but with a longlasting, non-propagating Ca^{2+} signal close to the nucleus (Estrada et al., 2001); the latter was attributed to Ins(1,4,5)*P*$_3$ production and the expression of types 1 and 3 Ins(1,4,5)*P*$_3$R (Estrada et al., 2001). Conklin et al. measured sparks in intercostal myotubes from RyR type 3-null embryonic mice (Conklin et al., 1999). Upon RyR stimulation using caffeine, the subcellular Ca^{2+} signals were significantly smaller and briefer in the knockout cells, and had faster time-to-peak values than in the wild-type cells (Conklin et al., 1999). However, using both type 1 and type 3 RyR-knockout mice, the same authors also reported that, in addition to the type 3 RyR, the type 1 RyR can also produce Ca^{2+} sparks in embryonic skeletal muscle cells (Conklin et al., 2000). Recent work in 3T3 fibroblasts also suggests a major role for cADPR and RyR (although the RyR subtype involved was not determined) in both amplification of localized Ca^{2+} signals and rapid propagation of Ca^{2+} waves through the cell body (Bruzzone et al., 2003).

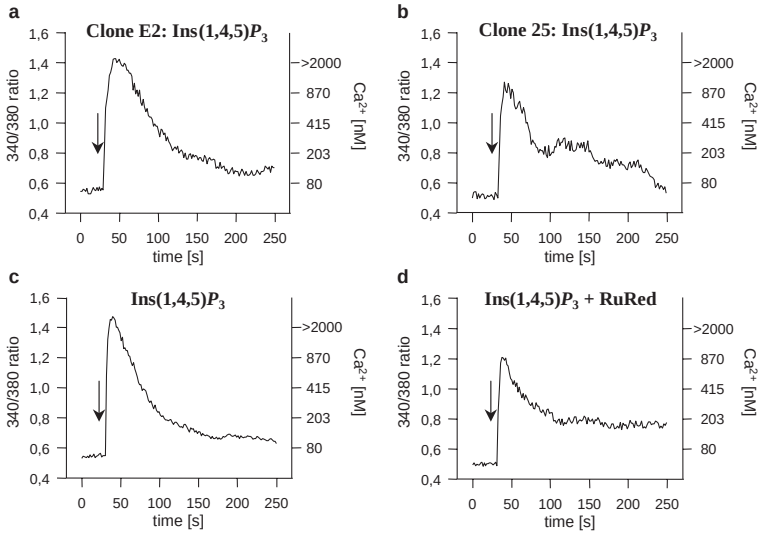

Fig. 5. Effect of type 3 RyR knockdown or RyR inhibition on global Ca^{2+} signaling upon activation of the Ins(1,4,5)*P*$_3$/Ca^{2+}-signaling system. T cells [control clone E2 (a) or type 3 RyR-knockdown clone 25 (b), or Jurkat T cells (c,d)] were loaded with Fura-2/AM and analyzed by single-cell Ca^{2+} imaging as described in the Materials and Methods. Ins(1,4,5)*P*$_3$ was microinjected (pipette concentration 4 μM) as indicated. Ruthenium Red (RuRed; pipette concentration 10 μM) was co-injected together with Ins(1,4,5)*P*$_3$. Data acquisition rate was 0.75 ratios/second. Characteristic tracings out of 5-9 cells are displayed.

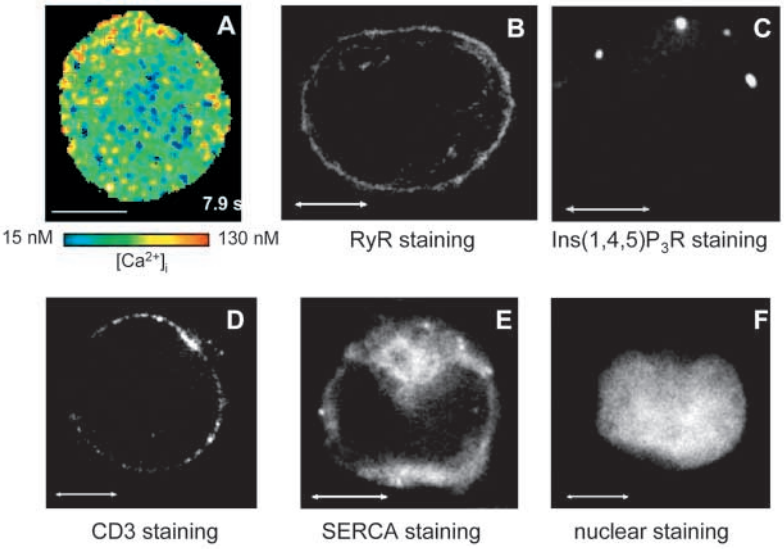

Fig. 6. Localization of organelles and Ca^{2+}-signaling proteins in T cells. T cells were fixed by p-formaldehyde, permeabilized by methanol (except for CD3 staining), and stained for RyR using BODIPY FL-X ryanodine (*n*=58; B), for Ins(1,4,5)*P*$_3$R using anti-Ins(1,4,5)*P*$_3$R antiserum and Rhodamine-conjugated secondary antibody (*n*=46; C), for CD3 using anti-CD3 antibody (OKT3) and a FITC-conjugated secondary antibody (*n*=17; D), for SERCA using BODIPY-thapsigargin (*n*=37; E), and for nuclei using Hoechst stain H33258 (*n*=37; F). Shown are characteristically stained single cells (bar, 5 μm). No or only weak fluorescence was seen in the control cells incubated without primary antibody or a surplus of ryanodine (10-fold) or thapsigargin (100-fold), respectively. All images were acquired from different individual cells. A representative confocal Ca^{2+} image (A; taken from Fig. 2Ab) facilitates comparison of protein and pacemaker signal localization.

In contrast to these findings, in RyR-knockdown portal vein smooth muscle cells obtained by microinjection of subtype-specific anti-RyR antisense oligonucleotides, no role for the type 3 RyR upon depolarization or stimulation by caffeine was observed under physiological Ca^{2+} concentrations (Coussin et al., 2000). However, under conditions of Ca^{2+} overload (superfusion with 10 mM Ca^{2+}), previous microinjection with antisense oligonucleotides directed against type 3 RyR reduced the global Ca^{2+} responses induced by phenylephrine and caffeine, but not spontaneous Ca^{2+} sparks (Mironneau et al., 2001).

Taken together, these data demonstrate for the first time under physiological conditions in T cells that the type 3 RyR is of crucial importance for both (1) the amplification of subcellular Ca^{2+} signals and (2) the spatiotemporal signal propagation during the pacemaker phase. The fact that knockdown of the type 3 RyR resulted in a reduced frequency rather than in a complete inhibition of these events highlights once more that T-cell Ca^{2+} signaling is a highly complex process obviously involving many players. However, among those known and unknown players, the type 3 RyR and cADPR do fulfill highly important roles in both the Ca^{2+} pacemaker phase (this study) and the longlasting Ca^{2+}-signaling phase (Schwarzmann et al., 2002; Guse et al., 1999).

This study was supported by the Deutsche Foschungsgemeinschaft (Grant no. GU 260/2-4 and 2-5 to A.H.G.), the Werner-Otto-Foundation (to A.H.G.), the Wellcome Trust (Biomedical Research Collaboration Grant no. 068065 to B.V.L.P. and A.H.G., and Programme Grant 060554 and Project Grant 055709 to B.V.L.P.), Research Funds of the Faculty of Medicine (Grant no. F-408-1 to A.H.G.), the National Natural Science Foundation of China (to L.-h.Z.) and the Deutsche Akademische Austauschdienst (Grant no. 314-vigoni-dr to A.H.G.).

References

Berg, I., Potter, B. V., Mayr, G. W. and Guse, A. H. (2000). Nicotinic acid adenine dinucleotide phosphate ($NAADP^+$) is an essential regulator of T-lymphocyte Ca^{2+}-signaling. *J. Cell Biol.* **150**, 581-588.

Berridge, M. J., Bootman, M. D. and Roderick, H. L. (2003). Calcium signalling: dynamics, homeostasis and remodelling. *Nat. Rev. Mol. Cell. Biol.* **4**, 517-529.

Bootman, M. D., Berridge, M. J. and Lipp, P. (1997a). Cooking with calcium: the recipes for composing global signals from elementary events. *Cell* **91**, 367-373.

Bootman, M., Niggli, E., Berridge, M. and Lipp, P. (1997b). Imaging the hierarchical Ca^{2+} signalling system in HeLa cells. *J. Physiol.* **499**, 307-314.

Bruzzone, S., Kunerth, S., Zocchi, E., De Flora, A. and Guse, A. H. (2003). Spatio-temporal propagation of Ca^{2+} signals by cyclic ADP-ribose in 3T3 cells stimulated via purinergic P2Y receptors, *J. Cell Biol.* 163, 837-845.

Conklin, M. W., Barone, V., Sorrentino, V. and Coronado, R. (1999). Contribution of ryanodine receptor type 3 to Ca^{2+} sparks in embryonic mouse skeletal muscle. *Biophys. J.* **77**, 1394-1403.

Conklin, M. W., Ahern, C. A., Vallejo, P., Sorrentino, V., Takeshima, H. and Coronado, R. (2000). Comparison of Ca^{2+} sparks produced independently by two ryanodine receptor isoforms (type 1 or type 3). *Biophys. J.* **78**, 1777-1785.

Coussin, F., Macrez, N., Morel, J. L. and Mironneau, J. (2000). Requirement of ryanodine receptor subtypes 1 and 2 for Ca^{2+}-induced Ca^{2+} release in vascular myocytes. *J. Biol. Chem.* **275**, 9596-9603.

da Silva, C. P. and Guse, A. H. (2000). Intracellular Ca^{2+} release mechanisms: multiple pathways having multiple functions within the same cell type? *Biochim. Biophys. Acta* **1498**, 122-133.

Estrada, M., Cardenas, C., Liberona, J. L., Carrasco, M. A., Mignery, G. A., Allen, P. D. and Jaimovich, E. (2001). Calcium transients in 1B5 myotubes lacking ryanodine receptors are related to inositol trisphosphate receptors. *J. Biol. Chem.* **276**, 22868-22874.

Galione, A. and Churchill, G. C. (2002). Interactions between calcium release pathways: multiple messengers and multiple stores. *Cell Calcium* **32**, 343-354.

Guse, A. H. (2000). Cyclic ADP-ribose. *J. Mol. Med.* **78**, 26-35.

Guse, A. H. (2002). Cyclic ADP-ribose (cADPR) and nicotinic acid adenine dinucleotide phosphate (NAADP): novel regulators of Ca^{2+}-signaling and cell function. *Curr. Mol. Med.* **2**, 273-282.

Guse, A. H., Roth, E. and Emmrich, F. (1993). Intracellular Ca^{2+} pools in Jurkat T-lymphocytes. *Biochem. J.* **291**, 447-451.

Guse, A. H., Goldwich, A., Weber, K. and Mayr, G. W. (1995). Non-radioactive, isomer-specific inositol phosphate mass determinations: high-performance liquid chromatography-micro-metal-dye detection strongly improves speed and sensitivity of analyses from cells and micro-enzyme assays. *J. Chromatogr. B. Biomed. Appl.* **672**, 189-198.

Guse, A. H., Berg, I., da Silva, C. P., Potter, B. V. and Mayr, G. W. (1997). Ca^{2+} entry induced by cyclic ADP-ribose in intact T-lymphocytes. *J. Biol. Chem.* **272**, 8546-8550.

Guse, A. H., da Silva, C. P., Berg, I., Skapenko, A. L., Weber, K., Heyer, P., Hohenegger, M., Ashamu, G. A., Schulze-Koops, H., Potter, B. V. et al. (1999). Regulation of calcium signalling in T lymphocytes by the second messenger cyclic ADP-ribose. *Nature* **398**, 70-73.

Guse, A. H., Tsygankov, A. Y., Weber, K. and Mayr, G. W. (2001). Transient tyrosine phosphorylation of human ryanodine receptor upon T cell stimulation. *J. Biol. Chem.* **276**, 34722-34727.

Huang, L. J., Zhou, Y. Y., Yuan, L., Min, J. M. and Zhang, L. H. (2002a). Chemical synthesis and calcium release activity of N-1-ether strand substituted cADPR mimic. Bioorg. Med. Chem. Lett. 12, 887-889.

Huang, L. J., Zhao, Y. Y., Yuan, L., Min, J. M. and Zhang, L. H. (2002b). Syntheses and calcium mobilizing evaluations of N^1-glycosyl substituted stable mimics of cyclic ADP-ribose. J. Med. Chem. 45, 5340-5352.

Jayaraman, T., Ondriasova, E., Ondrias, K., Harnick, D. J. and Marks, A. R. (1995). The inositol 1,4,5-trisphosphate receptor is essential for T-cell receptor signaling. *Proc. Natl. Acad. Sci. USA* **92**, 6007-6011.

Klein, M. G., Cheng, H., Santana, L. F., Jiang, Y. H., Lederer, W. J. and Schneider, M. F. (1996). Two mechanisms of quantized calcium release in skeletal muscle. *Nature* **379**, 455-458.

Kunerth, S., Koch-Nolte, F., Mayr, G. W. and Guse, A. H. (2003). Analysis of subcellular calcium signals in T-lymphocytes. *Cell. Signal.* **15**, 783-792.

Lipp, P. and Niggli, E. (1996). Submicroscopic calcium signals as fundamental events of excitation-contraction coupling in guinea-pig cardiac myocytes. *J. Physiol.* **492**, 31-38.

Mills, S. J. and Potter, B. V. L. (1996). Synthesis of D- and L-*myo* inositol 1,4,6-trisphosphate, regioisomers of a ubiquitous second messenger. *J. Org. Chem.* **61**, 8980-8987.

Mills, S. J., Riley, A. M., Murphy, C. T., Bullock, A. J., Westwick, J. and Potter, B. V. L. (1995). *myo*-Inositol 1,4,6-trisphosphorothioate and *myo*-inositol 1,3,4-trisphosphorothioate: new synthetic Ca^{2+}-mobilising partial agonists at the inositol 1,4,5-trisphosphate receptor. *Bioorg. Med. Chem. Lett.* **5**, 203-208.

Mironneau, J., Coussin, F., Jeyakumar, L. H., Fleischer, S., Mironneau, C. and Macrez, N. (2001). Contribution of ryanodine receptor subtype 3 to Ca^{2+} responses in Ca^{2+}-overloaded cultured rat portal vein myocytes. *J. Biol. Chem.* **276**, 11257-11264.

Murphy, C. T., Riley, A. M., Mills, S. J., Lindley, C. J., Potter, B. V. L. and Westwick, J. (2000). Myo-inositol 1,4,6-trisphosphorothioate and *myo*-inositol 1,3,6-trisphosphorothioate: partial agonists with very low intrinsic activity at the *myo*-inositol 1,4,5-trisphosphate receptor. *Mol. Pharmacol.* **57**, 595-601.

Rossi, D., Simeoni, I., Micheli, M., Bootman, M., Lipp, P., Allen, P. D. and Sorrentino, V. (2002). RyR1 and RyR3 isoforms provide distinct intracellular Ca^{2+} signals in HEK 293 cells. *J. Cell. Sci.* **115**, 2497-2504.

Schwarzmann, N., Kunerth, S., Weber, K., Mayr, G. W. and Guse, A. H. (2002). Knock-down of the type 3 ryanodine receptor impairs sustained Ca^{2+} signaling via the T cell receptor/CD3 complex. *J. Biol. Chem.* **277**, 50636-50642.

Thomas, D., Lipp, P., Tovey, S. C., Berridge, M. J., Li, W., Tsien, R. Y. and Bootman, M. D. (2000). Microscopic properties of elementary Ca^{2+} release sites in non-excitable cells. *Curr. Biol.* **10**, 8-15.

Thorn, P., Lawrie, A. M., Smith, P. M., Gallacher, D. V. and Petersen, O.

H. (1993). Local and global cytosolic Ca^{2+} oscillations in exocrine cells evoked by agonists and inositol trisphosphate. *Cell* **74**, 661-668.

Tsugorka, A., Rios, E. and Blatter, L. A. (1995). Imaging elementary events of calcium release in skeletal muscle cells. *Science* **269**, 1723-1726.

Tovey, S. C., de Smet, P., Lipp, P., Thomas, D., Young, K. W., Missiaen, L., De Smedt, H., Parys, J. B., Berridge, M. J., Thuring, J. et al. (2001). Calcium puffs are generic $InsP_3$-activated elementary calcium signals and are downregulated by prolonged hormonal stimulation to inhibit cellular calcium responses. *J. Cell. Sci.* **114**, 3979-3989.

Ward, C. W., Schneider, M. F., Castillo, D., Protasi, F., Wang, Y., Chen, S. R. and Allen, P. D. (2000). Expression of ryanodine receptor RyR3 produces Ca^{2+} sparks in dyspedic myotubes. *J. Physiol.* **525**, 91-103.

Yao, Y., Choi, J. and Parker, I. (1995). Quantal puffs of intracellular Ca^{2+} evoked by inositol trisphosphate in *Xenopus* oocytes. *J. Physiol.* **482**, 533-553.